
Mechanical regulation of localized and appositional bone formation around bone-interfacing implants

Craig A. Simmons, Shaker A. Meguid, Robert M. Pilliar

Institute of Biomaterials and Biomedical Engineering and Department of Mechanical and Industrial Engineering, University of Toronto, 170 College Street, Room 321, Toronto, Ontario M5S 3E3, Canada

Received 10 August 2000; accepted 5 October 2000

Abstract: The local mechanical environment around bone-interfacing implants determines, in large part, whether bone formation leading to functional osseointegration will occur. Previous attempts to relate local peri-implant tissue strains to tissue formation have not accounted for implant surface geometry, which has been shown to influence early tissue healing *in vivo*. Furthermore, the process by which mechanically regulated peri-implant bone formation occurs has not been considered previously. In the current study, we used a unit cell approach and the finite element method to predict the local tissue strains around porous-surfaced and plasma-sprayed implants, and compared the predictions to patterns of bone formation reported in earlier *in vivo* experiments. Based on the finite element predictions, we determined that appositional bone formation occurred when the magnitudes of the strain components at the tissue-host bone interface

were <8%. Localized, *de novo* bone formation occurred when the distortional tissue strains were less than approximately 3%. Based on these threshold tissue strains, we propose a mechanoregulatory model to relate local tissue strains to the process of peri-implant bone formation. The mechanoregulatory model is novel in that it predicts both appositional and localized bone formation and its predictions are dependent on implant surface geometry. The model provides initial criteria with which the osseointegration potential of bone-interfacing implants may be evaluated, particularly under conditions of immediate or early loading. © 2001 John Wiley & Sons, Inc. *J Biomed Mater Res* 55: 63–71, 2001

Key words: osseointegration; mechanoregulation; tissue differentiation; finite element analysis; porous-surfaced implant; plasma-sprayed implant

INTRODUCTION

The clinical success of bone-interfacing implants for orthopedic and dental applications is dependent on rigid fixation of the implants by mechanical interlock between the implant surface features and ingrown bone tissue. The mechanical environment experienced by the early healing tissue around these implants determines, in large part, whether bone formation and functional osseointegration will occur. However, efforts to quantify the relationship between mechanical stimuli and tissue formation have largely been unsuccessful. In experimental studies, measuring the local stresses and strains in the healing tissue is difficult, and consequently mechanical stimuli are described by the applied loading conditions, such as interfragmentary movement^{1–3} or implant relative displacement.^{4–9}

However, the local stresses and strains experienced by the healing tissue in a fracture gap or around an implant are dependent on many factors other than the loads applied globally. For bone-interfacing implants, these factors include the shape of the implant, the geometry of the implant surface, the mechanical interaction between the tissue and implant, and the site of implantation. Because of the multitude of variables, it has been impossible to define a relationship between mechanical parameters and peri-implant tissue formation that is applicable to a variety of implant designs and applications.

In an effort to determine the relationship between tissue strains and tissue formation, several investigators have estimated the local mechanical environment in the healing tissue at fracture sites or around bone-interfacing implants using computational models. From these studies, several theories relating the effects of specific mechanical stimuli to tissue formation have been proposed. Carter et al.¹⁰ hypothesized that progenitor cells within developing mesenchymal tissues that experience a loading history of low distortional strain and low compressive hydrostatic stress are more likely to become osteogenic, assuming an ad-

Correspondence to: R. M. Pilliar; e-mail: bob.pilliar@utoronto.ca

Contract grant sponsor: Medical Research Council of Canada

equate blood supply. However, if the healing tissue is exposed to excessive distortional strains, fibrogenesis results. On the other hand, significant compressive hydrostatic stresses and poor vascularity result in cartilage or fibrocartilage formation. Claes and Heigele¹¹ proposed a fracture healing theory similar to that of Carter et al., with the important distinction that new bone formation occurs only along fronts of existing bone or calcified tissue. Consistent with this appositional bone growth condition, they predicted that tissue formation is dependent on the magnitude of the strain components and hydrostatic pressure at the interface of the healing tissue and bone front. Specifically, Claes and Heigele predicted that intramembranous bone formation would take place at the bone front if the magnitudes of the strain components and hydrostatic pressure are $< 5\%$ and 0.15 MPa , respectively. Higher strains result in fibrogenesis and greater compressive hydrostatic pressure results in cartilage formation, possibly leading to endochondral ossification.

Attempts to relate early tissue formation to the local mechanical environment around bone-interfacing implants are limited to those by Prendergast, Huijskes, and coworkers.^{12–14} Using a biphasic material model to describe the healing tissue, they formulated a regulatory model in which tissue formation was controlled by shear strain in the solid phase of the tissue and the relative velocity between the fluid and solid components of the tissue. Based on their analyses, low tissue strains and low fluid velocities permit bone formation. However, their efforts to define the relationship between the mechanical parameters and tissue formation were limited by the assumptions made in their model, and in particular, failure to account for the implant surface geometry. Furthermore, they made no distinction between appositional bone formation from the host bone towards the implant surface and local *de novo* bone formation within the peri-implant tissue.

Recently, we showed that implant surface geometry influences early tissue formation and, as a result, the early mechanical stability of implants.¹⁵ Furthermore, we observed differences in the pattern of bone formation with different implant surface geometries at early times post-implantation in a rabbit femoral condyle model. For both nonfunctional Ti6Al4V sintered porous-surfaced and Ti plasma-sprayed implants, appositional bone formation from the host bone bed to the implant surface occurred. However, significant local bone formation within the porosity and irregularities of the implant surface structure was observed 8 days postimplantation only with the porous-surfaced design.^{15,16} This differential pattern of bone formation correlated with the local strains predicted by finite element analyses.¹⁶ These results suggest that implant surface geometry and the spatial distribution of new bone formation must be considered when investigat-

ing the relationship between mechanical stimuli and tissue formation.

The objective of our current study was to determine a quantitative relationship between tissue strain and peri-implant tissue formation. Using a unit cell approach and finite element analysis, we simulated two previously reported experimental studies in which patterns of bone formation were determined for implants with different surface geometries and different applied loads. Based on these analyses, we determined threshold strain levels for peri-implant bone formation and proposed a regulatory model that relates local tissue strains to patterns of tissue formation. This mechanoregulatory model is novel in that it predicts both appositional and local bone formation processes and its predictions are dependent on not only applied loads, but also implant surface geometry.

MATERIALS AND METHODS

Using finite element analysis, a unit cell approach and a homogenization technique (described below), we estimated the local tissue strains in the peri-implant region (the interface zone) for two cases. Our goal was to determine a relationship between local tissue strains and peri-implant tissue formation by comparing our model predictions for the local mechanical environment in the interface zone with observed patterns of bone formation. The two cases we considered were based on previously reported experimental studies in which bone formation was measured around implants with varying applied loads⁸ (Case 1) and different surface geometries¹⁵ (Case 2). Based on these analyses, we defined threshold strain levels for peri-implant bone formation.

Case 1

The first experimental study considered was that of Pilliar et al.,⁸ in which cylindrical porous-surfaced implants (Fig. 1) placed in canine mandibles were subjected to controlled loading shortly after implantation, before osseointegration had occurred. During the initial displacement-controlled loading period (for 6 or 7 days), relative displacements were applied to the tissue-implant interface using preselected shear displacements, ranging from 0 to $100\ \mu\text{m}$ (the path length through which a point at the tissue-implant interface was displaced). After the initial displacement-controlled loading period, the implants were displaced under load control at load levels that resulted in the initial prescribed displacements. The load-controlled displacements were imposed at regular intervals (30 cycles every second day at a frequency of $\sim 0.5\text{ Hz}$) for up to 3 weeks. The authors found that the degree of bone ingrowth into porous-surfaced implants was dependent on the level of applied displacement and there appeared to be a critical threshold shear displacement level of $50\ \mu\text{m}$ above which bone formation was inhibited. Furthermore, the degree of bone ingrowth de-

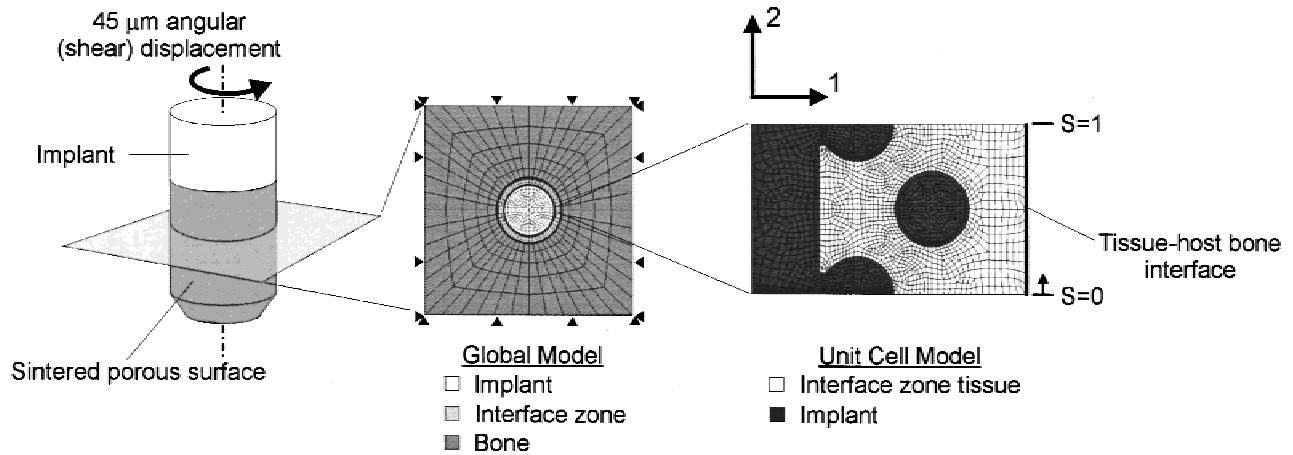


Figure 1. Finite element models used to simulate the experimental conditions for Case 1, a porous-surfaced implant subjected to $45\ \mu\text{m}$ of relative shear displacement, as described in Materials and Methods. The global model, representing a transverse cross-section of the porous-surfaced implant, was a two-dimensional, plane strain finite element model. The shear displacement was applied in the global model using prescribed nodal displacements along the junction of the implant and the homogenized interface zone. The unit cell model, which had an idealized geometry representing the porous-surfaced interface zone, was a two-dimensional, plane stress finite element model composed of 2228 four-noded elements. Relative displacement of the sintered particles with respect to one another was prevented by penalty constraints imposed in the unit cell model, thus simulating the relative stiffness of the surface structure. The normalized distance along the tissue–host bone interface, s , was measured from the bottom of the unit cell ($s = 0$) to the top of the unit cell ($s = 1$); this parameter was used in the characterization of the bone interface strains (Fig. 5).

creased from the outer region of the sintered porous surface structure toward the inner regions, suggesting that bone formation is primarily appositional in this case (Fig. 2). Because levels of displacement $>50\ \mu\text{m}$ inhibited bone ingrowth, this case represented a threshold condition and was used in the current study to define the strain threshold for peri-implant appositional bone formation.

We simulated the case of a sintered porous-surfaced implant subjected to an applied displacement of $45\ \mu\text{m}$ (which is just below the threshold displacement for bone formation with this implant system) to determine the threshold strain level for appositional bone formation. To simulate this case, we used the finite element method and a unit cell approach¹⁷ to predict the local strains in the healing interface zone tissue (i.e., before mineralization) around the implant. The unit cell approach was selected because it permitted

incorporation of the microstructural features of the implant interface into a global model of the entire implant. The basic premise of this method is that the composite being analyzed (in this case, the interface zone consisting of the implant surface features and ingrown granulation tissue) can be modelled by a series of repeating unit cells (UCs) that are representative of the microstructure (Fig. 1). The UC for the sintered porous surface had an idealized geometry that was based on the key characteristics of the implants used in the experiments by Pilliar et al.,⁸ including volume porosity, pore size, interface zone width, and allowance for mechanical interlock between the early repair tissue and implant surface features (Fig. 1).

We have used the unit cell method and homogenization technique previously to predict the local mechanical environment around porous-surfaced and plasma-sprayed implants.¹⁶ Our approach in the current study differed slightly because the geometry and loading condition considered in Case 1 resulted in large (i.e., finite), nonuniform strains across the interface zone. The linearized homogenization method assumes a constant, infinitesimal strain within the homogenized interface zone tissue in its prediction of the local strains, and therefore was inappropriate for this application. Instead, the local tissue strains were determined using a cut-boundary displacement method¹⁸ and a nonlinear finite element analysis, which accounted for geometric nonlinearities resulting from large rotations and finite strains. In this analysis, the unit cell model represented a region of the global model (the interface zone in this case), and the boundary of the unit cell model represented a cut through the global model. Nodal displacements were applied tangential to the implant interface in the global finite element model to simulate the applied loading conditions in the canine micromovement experiments. The displacements predicted by the global model along the cut boundary were then interpolated

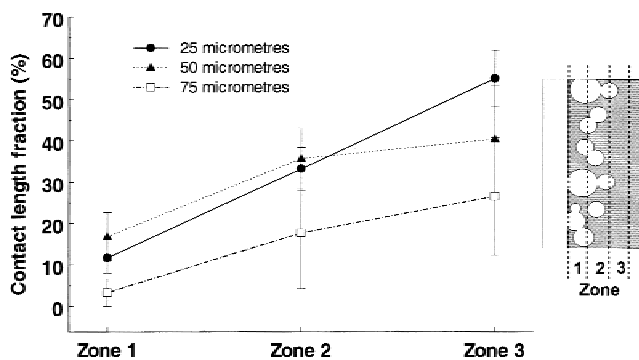


Figure 2. Bone ingrowth (quantified as contact length fraction) into the mesial aspect of the surface structure of porous-surfaced implants for various levels of applied shear displacement (based on data from Pilliar et al.⁹). Data are presented as mean \pm standard error.

for each node on the unit cell boundary using the element shape functions, and then applied as boundary conditions in the unit cell model. The unit cell model was then analyzed using a nonlinear finite element analysis to determine the local strains. Therefore, this technique accounted for non-uniform, finite strains within the global interface zone and the unit cell. All modeling was performed using a custom software package written using MATLAB (The Mathworks, Inc., Natick, MA) in conjunction with a commercial finite element package (ANSYS 5.4; Ansys, Inc., Canonsburg, PA).

In the global and unit cell finite element models, the implant material, homogenized interface zone, interface zone tissue, and surrounding bone bed were modeled as homogeneous, linear elastic materials (Table I). The interface zone tissue properties represented early, premineralized repair tissue and were based on values determined by a computational model¹⁹ of implant pull-out tests, albeit for a rabbit femoral implant site at 4 days postimplantation.¹⁵ The homogenized or effective properties of the interface zone in the global model were predicted by finite element analysis and the homogenization method.¹⁶ It was assumed that the metal and tissue were bonded perfectly and that the tissue infiltrated the porosity or irregularities of the implant surfaces fully.

Case 2

The second experimental study considered was that of Simmons et al.,¹⁵ in which it was found that mineralization of the peri-implant healing tissue was more rapid around nonfunctional sintered Ti6Al4V porous-surfaced implants than around nonfunctional Ti plasma-sprayed implants. Quantitative image analysis demonstrated that the greatest differences in initial bone formation (i.e., 8 days postimplantation) between the two implant designs occurred within the outer zone of the surface of the implant (the surface zone) (Fig. 3), an area that is “strain-protected” to a greater extent with the porous-surfaced design according to finite element predictions.¹⁶ Furthermore, local *de novo* mineralized tissue formation occurred to a greater extent in the surface zone

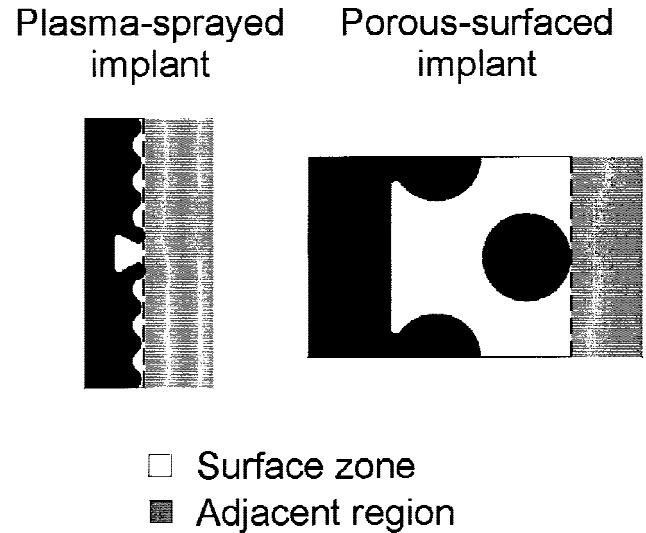


Figure 3. The local tissue strains for Case 2 were determined for (a) the surface zone, in which local *de novo* bone formation was observed in the animal studies,^{15,16} and (b) the adjacent region, where minimal local bone formation was observed.

than in the adjacent region peripheral to the implant, particularly with the porous-surfaced design. These results suggest that the differences in local tissue strains between the surface zone and adjacent region provide an estimate of the threshold matrix strain for local bone formation. In the current study, we extended the analysis from an earlier computational study¹⁶ to predict the threshold matrix strain for local tissue mineralization. Specifically, we reanalyzed the data from Simmons et al.¹⁶ to compare the local tissue strains within the surface zones of the porous-surfaced and plasma-sprayed implants with the tissue strains in the regions adjacent to the surface structures (i.e., between the host bone and implant surface structure) (Fig. 3).

Interpretation of local strain predictions

We interpreted the local strain fields predicted by our computational analyses according to the theories proposed by Carter et al.¹⁰ and Claes and Heigele¹¹ for mechanically regulated tissue formation, theories that were developed based primarily on observations made during fracture healing. Carter et al.’s theory relates tissue strain parameters to bone, fibrous tissue, or cartilage formation within a pluripotent mesenchymal tissue, as described previously. Within the context of peri-implant tissue formation, we interpreted this as a model for local bone formation within the tissue matrix. Therefore, for both cases analyzed, we determined the distortional (octahedral) and volumetric (hydrostatic) tissue strains¹⁶ (the parameters proposed by Carter et al.¹⁰ to influence tissue formation) within the bulk of the interface zone tissue in the unit cell models.

Claes and Heigele¹¹ hypothesized that mechanically regulated bone formation occurs on existing bone surfaces. In the context of peri-implant tissue formation, this describes ap-

TABLE I
Elastic Constants Used in the Finite Element Models

Material	Elastic Modulus, E	Poisson’s Ratio, ν
Titanium	110 GPa	0.33
Trabecular bone*	500 MPa	0.4
Interface zone tissue [†]	1 MPa	0.47
Homogenized (global) interface zone [‡]	$E_1 = 3.59$ MPa $E_2 = 28.2$ GPa $G_{12} = 1.18$ MPa	$\nu_{12} = 3.9 \times 10^{-5}$ $\nu_{21} = 0.306$

*Based on representative values from Keaveny and Hayes.⁴²

[†]The properties of the interface zone tissue in the local (unit cell) models were estimated from mechanical pull-out tests (refer to text).

[‡]The transversely isotropic properties of the homogenized interface zone in the global model were based on predictions from finite element analysis and homogenization methods.¹⁶ Refer to Figure 1 for definitions of the 1- and 2-directions.

positional bone growth from the host bone bed towards the implant surface. Therefore, for Case 1 we determined the local transverse (perpendicular to the tissue–host bone interface) and longitudinal (parallel to the tissue–host bone interface) strain components and the local hydrostatic pressure at nodes along the tissue–bone interface in the unit cell models. As described previously, these parameters were proposed by Claes and Heigele¹¹ to predict tissue formation on existing bone surfaces.

RESULTS

Local tissue strains predicted for Case 1

For the porous-surfaced implant and an applied shear displacement of 45 μm , the global equivalent strain varied nonlinearly across the interface zone. The global strain was the lowest near the implant surface (6.7%) and the tissue–bone interface (6.6%), and highest near the middle of the interface zone (12.7%). However, because of the structural features of the interface zone, a wide range of local distortional and volumetric tissue strains was predicted (Fig. 4). Furthermore, the spatial distribution of the local tissue strains was significantly different from that predicted by the global model (Fig. 5). For the 45- μm applied displacement, the median distortional tissue strain was 17%, but varied significantly throughout the interface zone. Minimal local bone formation was observed in this case,⁸ suggesting that the distortional strains predicted for the majority of the peri-implant tissue in this case are above the threshold for bone formation.

Compared to the distortional tissue strains, the magnitudes of the volumetric tissue strains were lower, with a median value of 0.4%, and 87% of the tissue experiencing volumetric tissue strains between -5% and $+5\%$ (Fig. 4). No cartilage formation was observed in the animal model studies for this loading

condition,⁸ suggesting that if volumetric strain (or equivalently, hydrostatic stress) predicts chondrogenesis,¹⁰ then the volumetric strains predicted for this case are subthreshold.

We also calculated the local longitudinal and transverse strain components and the local hydrostatic pressure at the tissue–bone interface as predictors of appositional bone formation. For the porous-surfaced implant and an applied shear displacement of 45 μm , the transverse strains varied between -8% and $+2\%$ and the longitudinal strains were $<1\%$ along the bone surface (Fig. 6). The hydrostatic pressure fluctuated along the bone surface, with a maximum value of -0.13 MPa (Fig. 6). Bone formation for this loading condition in the animal experiments was primarily appositional, and because the applied displacement in this case was near the threshold for bone formation, the predicted tissue–bone interface strains estimate the threshold values for appositional bone formation.

Local tissue strains predicted for Case 2

Within the surface zones of the porous-surfaced and plasma-sprayed implants, the median distortional tissue strains were 0.68% and 1.46%, respectively, and were generally $<3\%$ (Fig. 7 and 8). In the adjacent region between the host bone and implant surface structure, the median distortional tissue strains were 5.3% and 4.3% for the plasma-sprayed and porous-surfaced implants, respectively (Fig. 7 and 8). In the animal experiments, local bone formation was confined primarily to the surface zones of the porous-surfaced and plasma-sprayed implants, with little *de novo* bone formation in the adjacent regions 8 days postimplantation (although appositional bone formation did occur).^{15,16} The differences in the distortional strains predicted for these two regions suggest a threshold value

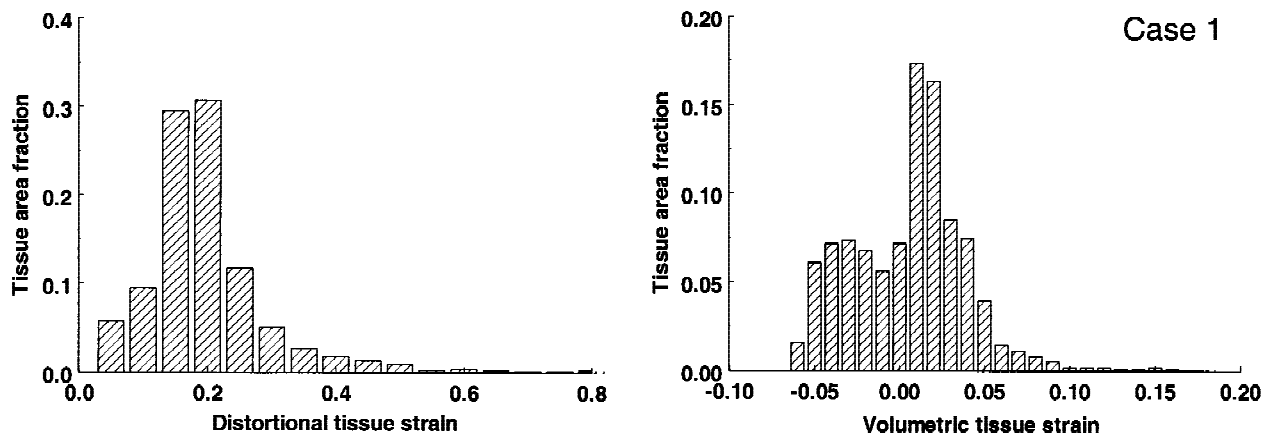


Figure 4. Histograms of the area fraction of interface zone tissue experiencing various levels of distortional and volumetric strains for a porous-surfaced implant subjected to 45 μm of relative shear displacement (Case 1).

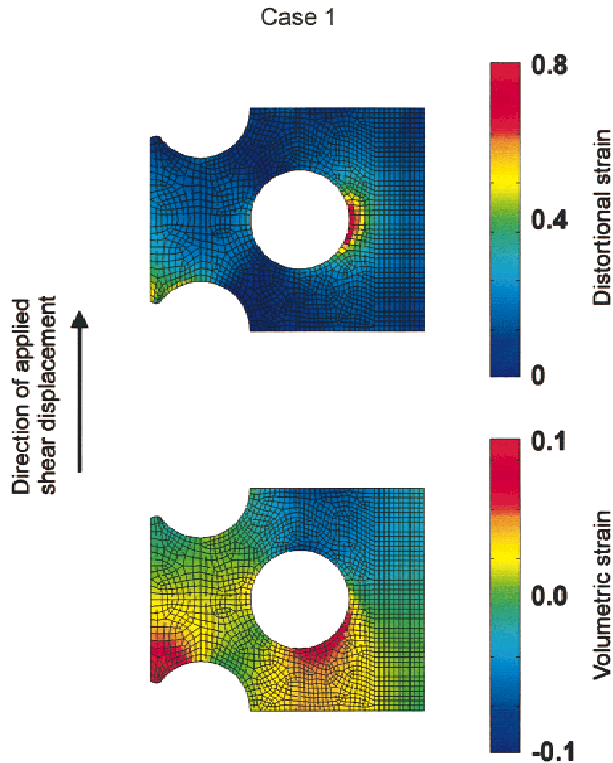


Figure 5. Field plots of the local distortional and volumetric tissue strains around a porous-surfaced implant subjected to $45\ \mu\text{m}$ of relative shear displacement (Case 1).

of approximately 3%, above which local bone formation is inhibited. No cartilage was observed in the animal experiments,¹⁵ indicating that the volumetric strains predicted for this case ($<5\%$; data not shown) do not induce chondrogenesis.

DISCUSSION

The objective of this study was to investigate the relationship between the local mechanical environment and tissue formation around bone-interfacing

implants. Gross characterizations of threshold mechanical stimuli for peri-implant bone formation (such as micromovement) are implant specific, surface geometry specific, and site specific. Therefore, a more universal criterion, such as local tissue strain, is necessary to evaluate orthopedic and dental implant designs and rehabilitation protocols that promote more rapid and reliable osseointegration. Furthermore, identifying the relationship between tissue strain and tissue formation has important implications to the design of fracture repair devices and engineered skeletal tissues.

Based on comparisons of local tissue strains predicted using a unit cell approach and the finite element method to patterns of bone formation observed experimentally, we estimated threshold levels of local tissue strains for appositional and local peri-implant bone formation. These strain thresholds are the basis of a mechanoregulatory model we propose to relate the local mechanical environment around bone-interfacing implants to processes of bone formation (Fig. 9). Following the fracture healing theories of Carter et al.¹⁰ and Claes and Heigele,¹¹ we use distortional tissue strain as a predictor of localized bone formation within the interface zone tissue and the magnitudes of the longitudinal and transverse strain components at the tissue–bone interface (referred to as bone interface strains) as predictors of appositional bone growth. The bone formation processes are dependent on these two predictors, with both appositional and localized bone formation occurring only when the distortional tissue strain is $<3\%$ and the magnitudes of the bone interface strains are $<8\%$. The current model accounts only for bone or fibrous tissue formation, because those were the only tissue types observed in the experiments that were simulated. If large hydrostatic stresses cause cartilage or fibrocartilage formation, then based on the computational

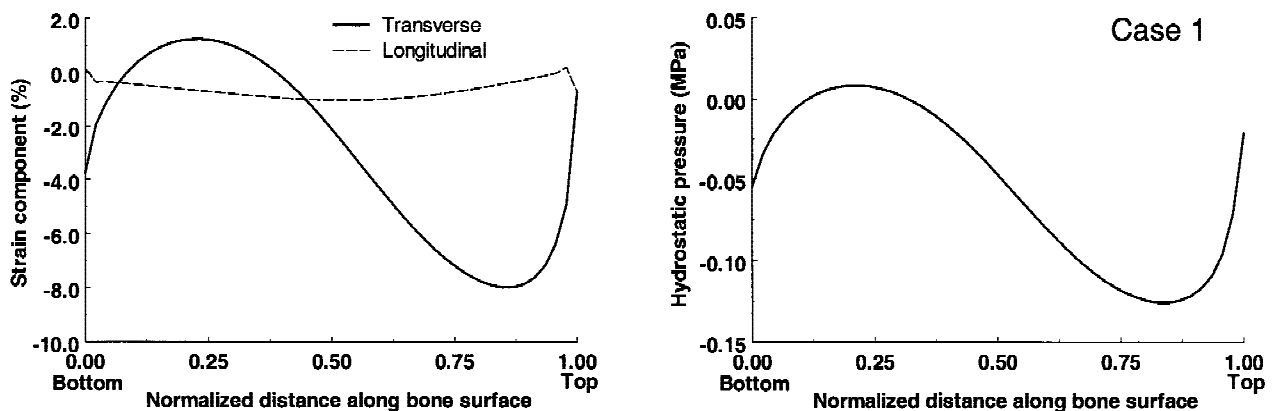


Figure 6. Local strain components and hydrostatic pressures along the tissue–host bone interface predicted for a porous-surfaced implant subjected to $45\ \mu\text{m}$ of relative shear displacement (Case 1). The normalized distance along the bone surface is defined in Figure 1.

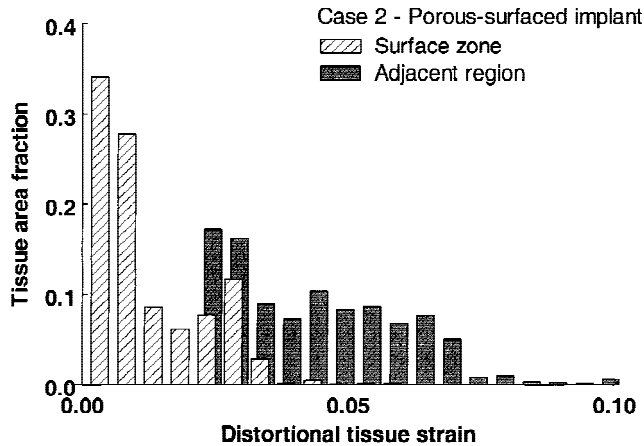


Figure 7. Histograms of the area fraction of interface zone tissue experiencing various levels of distortional strain for the porous-surfaced implant in Case 2. The tissue in the surface structure region, where local bone formation was observed in the animal experiments,^{15,16} experienced generally lower distortional strains than the tissue in the adjacent region. The surface structure and adjacent regions are defined in Figure 2.

model predictions in this study, the magnitude of the hydrostatic stress threshold is >0.13 MPa. Although our analysis considered only a single time point (i.e., 4 days postimplantation), representing the period before tissue mineralization, the mechanoregulatory model could be applied in an iterative manner to predict spatial and temporal patterns of bone formation.

The threshold strains for bone formation predicted in this study are consistent with data from several *in vivo* and *in vitro* experimental studies, thus supporting the initial validity of the model and the analysis. For instance, earlier studies using computational, *in vitro*, and *in vivo* models have estimated the critical tissue or

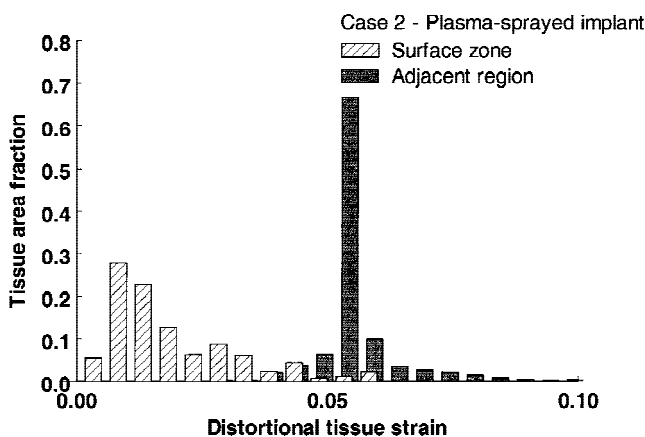


Figure 8. Histograms of the area fraction of interface zone tissue experiencing various levels of distortional strain for the plasma-sprayed implant in Case 2. As with the porous-surfaced implant, the tissue in the surface structure region experienced lower distortional strains than the tissue in the adjacent region. The surface structure and adjacent regions are defined in Figure 2.

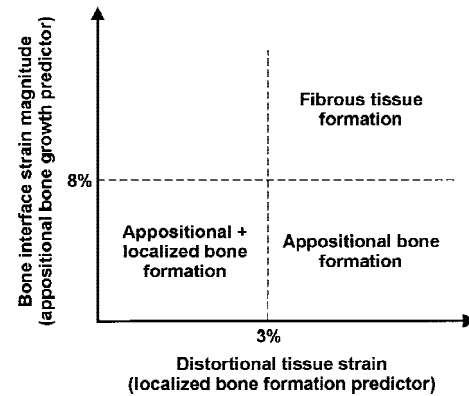


Figure 9. Mechanoregulatory model proposed for tissue formation around bone-interfacing implants. The threshold strains for bone formation were determined from the finite element simulations of *in vivo* experiments. The model predicts appositional bone formation if the bone interface strain magnitudes are $<8\%$ and localized bone formation within the healing tissue matrix if the distortional tissue strains are less than approximately 3% . The model is applicable in cases in which the magnitude of the hydrostatic pressure at the tissue–bone interface and within the tissue matrix is less than at least 0.13 MPa; larger compressive hydrostatic stresses may promote cartilage or fibrocartilage formation.

matrix strain level above which osteoblast differentiation and bone formation are inhibited to be on the order of $1\text{--}10\%$ (quantified using a variety of strain measures).^{11,14,20–23} Our predictions for the threshold distortional strain for local bone formation and the threshold strain magnitude for appositional bone formation are within this range. The critical compressive hydrostatic stress magnitude above which cartilage formation is stimulated has been estimated to be between 0.15 and 2 MPa.^{11,20,23} The hydrostatic stress threshold predicted in our analysis was >0.13 MPa, consistent with earlier studies.

The mechanoregulatory model is novel in two respects. First, it predicts appositional and local bone formation processes, both of which have been observed experimentally around bone-interfacing implants.^{15,24–26} Osseointegration of an implant may result from bone formation by either process. However, the rate at which osseointegration occurs may depend on whether both appositional and localized bone formation are occurring (versus appositional alone), as suggested by previous finite element studies.¹⁶ The bone formation processes predicted by the model assume that the tissue and implant surface are bonded rigidly. Although this is a reasonable initial approximation of the situation *in vivo*,¹⁶ the model does not account for failure of the implant–tissue interface during the early healing period, which would occur with excessive loading of an implant. Interface failure would decouple the implant from the interface zone tissue, thereby altering the load transfer mechanisms from the implant to the surrounding tissue. How this

decoupling would influence peri-implant tissue formation is difficult to predict, and future modeling efforts should consider alternate interface conditions, such as contact and possible failure of the interface. The challenge in incorporating interface failure conditions is that the mechanical characteristics of the tissue-metal interface are poorly characterized and difficult to determine experimentally.

The second novel aspect of the mechanoregulatory model is that its predictions are dependent on the implant surface geometry, consistent with experimental observations.¹⁵ The effect of surface geometry on the mechanical regulation of peri-implant tissue formation has not been considered previously,^{12-14,20} although it clearly influences the magnitudes and distributions of the local tissue strains, as shown in the current study and by others.^{16,27-29} The clinical implication of the surface geometry dependence is twofold. First, certain implant designs may be preferable to others in terms of their ability to osseointegrate more rapidly, leading to shorter rehabilitation times. Second, certain designs may tolerate higher levels of micromovement or applied loading, and therefore would be less vulnerable to adverse loading during the healing period.

Although the mechanoregulatory model predictions are consistent with experimental observations, it is important to note that the model accounts only for the regulation of tissue formation by mechanical factors, and neglects other stimuli associated with wound healing, although they may be more important than mechanical stimuli in initial bone formation.³⁰ For instance, the poor clinical results with cementless implants in elderly patients suggest that hormonal and age-related factors play an important role in determining osseointegration potential. Also, nonmechanical antiangiogenic factors are not accounted for in the model, although an adequate blood supply is "probably the most absolute requirement for new bone formation."³¹ In addition, implant surface geometry may influence tissue formation through means other than those proposed here, such as directly affecting cell behavior (see, for instance, Boyan et al.³²). It is clear, however, that mechanical forces can perturb the initial tissue formation process. It is likely that because of the nonmechanical factors, instead of a single critical strain threshold for peri-implant bone formation, there is a range of strains that is dependent on several factors, including age, health status, and implantation site. The model is also limited in that it is phenomenological and cannot elucidate the specific details and mechanisms that regulate tissue formation mechanically. Nonetheless, the phenomenological approach can provide valuable insights into the process of tissue formation and can suggest avenues for future basic research. Furthermore, the results from these analyses may have practical clinical value.

We interpreted the computational model results using two theories that have been proposed to relate tissue strains and tissue formation during fracture healing. These theories were selected because peri-implant tissue formation has been described as a process analogous to fracture repair.³³ The theories were also compatible with the single-phase, isotropic material description of the early healing tissue in the current analysis. Because the material model was not biphasic, we were unable to consider the effects of fluid flow. It is difficult to predict how the tissue strain predictions may have changed had a poroelastic or biphasic material model been implemented, and the literature provides conflicting opinions.^{12,34,35} It is likely, however, that there would be a time-dependency of the local tissue strains, a feature not captured with the linear, elastic model and quasi-static loads applied in the current analysis. Furthermore, fluid flow-induced shear stress may be an important mechanoregulatory signal in initial bone formation,^{13,36-40} and therefore future studies need to incorporate more realistic material descriptions. However, as illustrated in this study, the microstructural features of the implant surface influence the local tissue strains significantly, and therefore the challenge is to incorporate more complex material descriptions into finite element modeling approaches that account for the implant surface geometry. Recent work by Wu et al.⁴¹ on cartilage micromechanics provides a theoretical basis for the development of biphasic micromechanical models of the tissue-implant interface using a unit cell approach.

In conclusion, we have proposed a quantitative model for the mechanical regulation of peri-implant tissue formation based on predictions of local tissue strains made using the finite element method and a unit cell approach. The model is novel in that it predicts both appositional and localized bone formation processes and its predictions depend on the implant surface geometry (consistent with experimental observations). The model provides initial criteria by which the osseointegration potential of a variety of bone-interfacing implant designs, fracture fixation devices, and engineered skeletal tissue constructs may be evaluated, particularly under conditions of immediate or early mechanical loading.

References

1. Sarmiento A, Schaeffer JF, Beckerman L, Latta LL, Enis JE. Fracture healing in rat femora as affected by functional weight-bearing. *J Bone Jt Surg [Am]* 1977;59-A:369-375.
2. Goodship AE, Kenwright J. The influence of induced micromovement upon the healing of experimental tibial fractures. *J Bone Jt Surg [Br]* 1985;67-B:650-655.
3. Li G, Simpson AHRW, Kenwright J, Triffitt JT. Assessment of cell proliferation in regenerating bone during distraction osteogenesis at different distraction rates. *J Orthop Res* 1997;15:765-772.

4. Bragdon CR, Burke DW, Lowenstein JD, O'Connor DO, Ramamurti B, Jasty M, Harris WH. Differences in stiffness of the interface between a cementless porous implant and cancellous bone in vivo in dogs due to varying amounts of implant motion. *J Arthroplasty* 1996;11:945-951.
5. Hollis JM, Hoffman OE, Stewart CL, Flahiff CM, Nelson C. Effect of micromotion on ingrowth into porous coated implants using a transcortical model. Fourth World Biomaterials Congress; 1992 April 24-28; Berlin, Germany. p 258.
6. Søballe K, Hansen ES, B.-Rasmussen H, Jørgensen PH, Bünger C. Tissue ingrowth into titanium and hydroxyapatite-coated implants during stable and unstable conditions. *J Orthop Res* 1992;10:285-299.
7. Søballe K, Brockstedt-Rasmussen H, Hansen ES, Bünger C. Hydroxyapatite coating modifies implant membrane formation. *Acta Orthop Scand* 1992;63:128-140.
8. Pilliar RM, Deporter DA, Watson P. Tissue-implant interface: Micromovement effects. In: Vincenzini P, editor. *Materials in clinical applications*. Faenza, Italy: Techna; 1995. p 569-579.
9. Pilliar RM, Deporter DA, Watson PA, Abdulla D, Valiquette N, Lindsay D. Quantitative determination of relative movement effects on bone ingrowth with porous-coated implants. Fifth World Biomaterials Congress; 1996 May 29-June 2; Toronto, Ontario. p 261.
10. Carter DR, Beaupre GS, Giori NJ, Helms JA. Mechanobiology of skeletal regeneration. *Clin Orthop Rel Res* 1998;355(Suppl):S41-S55.
11. Claes LE, Heigele CA. Magnitudes of local stress and strain along bony surfaces predict the course and type of fracture healing. *J Biomech* 1999;32:255-266.
12. Prendergast PJ, Huiskes R. Finite element analysis of fibrous tissue morphogenesis: A study of the osteogenic index with a biphasic approach. *Mech Comp Mater* 1996;32:144-150.
13. Prendergast PJ, Huiskes R, Søballe K. Biophysical stimuli on cells during tissue differentiation at implant interfaces. *J Biomech* 1997;30:539-548.
14. Huiskes R, Driel WDV, Prendergast PJ, Søballe K. A biomechanical regulatory model for periprosthetic fibrous-tissue differentiation. *J Mater Sci Mater Med* 1997;8:785-788.
15. Simmons CA, Valiquette N, Pilliar RM. Osseointegration of sintered porous-surfaced and plasma-spray coated implants: An animal model study of early post-implantation healing response and mechanical stability. *J Biomed Mater Res* 1999;47:127-138.
16. Simmons CA, Meguid SA, Pilliar RM. Differences in osseointegration rate due to implant surface geometry can be explained by local tissue strains. *J Orthop Res* (in press).
17. Hollister SJ, Kikuchi N. A comparison of homogenization and standard mechanics analyses for periodic porous composites. *Comput Mech* 1992;10:73-95.
18. ANSYS Inc., editor. *Submodeling*. In: ANSYS advanced analysis techniques. Canonsburg, PA: SAS IP, Inc.; 1997.
19. Simmons CA. *Modelling and characterization of mechanically regulated tissue formation around bone-interfacing implants*. Ph.D. thesis, University of Toronto; 2000.
20. Giori NJ, Ryd L, Carter DR. Mechanical influences on tissue differentiation at bone-cement interfaces. *J Arthroplasty* 1995;10:514-522.
21. Jones DB, Nolte H, Scholübbbers J-G, Turner E, Veltel D. Biochemical signal transduction of mechanical strain in osteoblast-like cells. *Biomaterials* 1991;12:101-110.
22. Meyer U, Wiesmann HP, Kruse-Lösler B, Handschel J, Stratmann U, Joos U. Strain-related bone remodeling in distraction osteogenesis of the mandible. *Plast Recon Surg* 1999;103:800-807.
23. Tägil M, Aspenberg P. Cartilage induction by controlled mechanical stimulation in vivo. *J Orthop Res* 1999;17:200-204.
24. Osborn JF, Newsley H. Dynamic aspects of the implant-bone interface. In: Heimke G, editor. *Dental implants: Materials and systems*. Munich: Carl Hanser; 1980. p 111-123.
25. Spector M. Bone ingrowth into porous polymers. In: Williams DF, editor. *Biocompatibility of orthopedic implants*. Boca Raton: CRC Press, 1982. p 55-88.
26. Pilliar RM, Lee JM, Maniopoulos C. Observations on the effect of movement on bone ingrowth into porous-surfaced implants. *Clin Orthop Rel Res* 1986;208:108-113.
27. Ko CC, Kohn DH, Hollister SJ. Micromechanics of implant/tissue interfaces. *J Oral Implant* 1992;18:220-230.
28. Kohn DH, Ko C-C, Hollister SJ. Effect of tissue modulus, symmetry and fibrous tissue on the local properties of a porous coating/tissue interfacial zone. *Orthopaedic Research Society*; 1993 Feb 15-18; San Francisco, CA. p 223.
29. Pedersen DR, Brown TD, Brand RA. Interstitial bone stress distributions accompanying ingrowth of a screen-like prosthesis anchorage layer. *J Biomech* 1991;24:1131-1142.
30. Hollister SJ, Guldberg RE, Kuelske CL, Caldwell NJ, Richards M, Goldstein SA. Relative effects of wound healing and mechanical stimulus on early bone response to porous-coated implants. *J Orthop Res* 1996;14:654-662.
31. Aronson J. Experimental assessment of bone regenerate quality during distraction osteogenesis. In: Brighton CT, Friedlaender G, Lane JM, editors. *Bone formation and repair*. Rosemont, IL: American Academy of Orthopaedic Surgeons; 1994. p 441-463.
32. Boyan BD, Hummert TW, Dean DD, Schwartz Z. Role of material surfaces in regulating bone and cartilage cell response. *Biomaterials* 1996;17:137-146.
33. Galante JO. The biological basis of bone ingrowth in titanium fiber composites. In: Harris WH, editor. *Advanced concepts in total hip replacement*. Thorofare, NJ: SLACK, Inc.; 1985. p 137-158.
34. Carter DR, Beaupré GS. Linear elastic and poroelastic models of cartilage can produce comparable stress results: A comment on Tanck et al. (*J Biomech* 32:153-161, 1999). *J Biomech* 1999;32:1255-1256.
35. Tanck E, van Driel WD, Blankevoort L, Huiskes R, Hagen JW, Burger EH. Response to Beaupré and Carter. *J Biomech* 1999;32:1257.
36. Smalt R, Mitchell FT, Howard RL, Chambers TJ. Induction of NO and prostaglandin E₂ in osteoblasts by wall-shear stress but not mechanical strain. *Am J Physiol* 1997;273:E751-E758.
37. McAllister TN, Frangos JA. Steady and transient fluid shear stress stimulate NO release in osteoblasts through distinct biochemical pathways. *J Bone Miner Res* 1999;14:930-936.
38. Hillsley MV, Frangos JA. Alkaline phosphatase in osteoblasts is down-regulated by pulsatile fluid flow. *Calcif Tissue Int* 1997;60:48-53.
39. Jacobs CR, Yellowley CE, Davis BR, Zhou Z, Cimbala JM, Donahue HJ. Differential effect of steady versus oscillating flow on bone cells. *J Biomech* 1998;31:969-976.
40. Owan I, Burr DB, Turner CH, Qiu J, Tu Y, Onyia JE, Duncan RL. Mechanotransduction in bone: osteoblasts are more responsive to fluid forces than mechanical strain. *Am J Physiol* 1997;273:C810-C815.
41. Wu JZ, Herzog W, Epstein M. Modelling of location- and time-dependent deformation of chondrocytes during cartilage loading. *J Biomech* 1999;32:563-572.
42. Keaveny TM, Hayes WC. Mechanical properties of cortical and trabecular bone. In: Hall BK, editor. *Bone*. Boca Raton: CRC Press; 1993. p 285-344.